Dissolution of unirradiated MOX fuel in the presence of magnetite and chukanovite

Nuclear Materials and Energy 47 (2026) 102148

Contents lists available at ScienceDirect

Nuclear Materials and Energy

journal homepage: www.elsevier.com/locate/nme

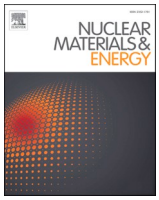

Dissolution of unirradiated MOX fuel in the presence of magnetite and chukanovite

M. Saleh [a,*], E. Darwish [a], M. Hedberg [a], P.L. Tam [b], K. Spahiu [a,c], C. Ekberg [a]

[a] Nuclear Chemistry / Industrial Materials Recycling, Chalmers University of Technology, SE-412 96 Gothenburg, Sweden
[b] Department of Industrial and Materials Science, Chalmers University of Technology, SE-412 96 Gothenburg, Sweden
[c] Swedish Nuclear Fuel and Waste Management Co., SE-101 24 Stockholm, Sweden

ARTICLE INFO

Keywords:
MOX fuel
Groundwater
Alpha radiolysis
Fuel dissolution
Magnetite
Chukanovite

ABSTRACT

In all European concepts for deep geological repositories of spent nuclear fuel, massive canisters with cast iron inserts are designed to prevent early interaction between the spent nuclear fuel and groundwater. Should a canister breach occur, corrosion of the fuel would take place at repository depths of several hundred meters where the surrounding groundwater is generally anoxic. The radiation field surrounding the fuel alters local redox conditions through water radiolysis. Under such conditions, fuel corrosion is anticipated to proceed simultaneously with anoxic iron corrosion. When all iron is corroded, iron corrosion products will be present for very long times in the near field of a repository and thus buffer the redox conditions in the near field. By using a MOX fuel pellet with an extremely high alpha field, we can test the effects of iron corrosion products on fuel dissolution considering that the very old fuel they will contact in the repository has orders of magnitude lower alpha dose rates.

In this study, two leaching experiments were conducted on unirradiated MOX fuel pellets containing 10 wt% plutonium (specific alpha activity: 1.79 GBq/g) under an argon atmosphere in simulated granitic groundwater representative of the Forsmark site in Sweden. The experiments were performed in the presence of magnetite and synthesized chukanovite to assess their influence on the corrosion and leaching behaviour of the unirradiated MOX fuel. A strong inhibiting effect on fuel dissolution was noted for chukanovite, while magnetite could not counteract the radiolytic dissolution of the unirradiated MOX pellet.

1. Introduction

Understanding the mechanisms that govern the stability of spent nuclear fuel under repository conditions is a key factor in evaluating the long-term safety of deep geological disposal systems. The dissolution of the UO_2(s)-based fuel matrix largely determines the potential release of radionuclides once the protective canister barrier is compromised [1]. Although reducing groundwater environments, such as those anticipated in crystalline bedrock, are expected to maintain UO_2(s) in a thermodynamically stable state with very low solubility [2], the radiation field surrounding the fuel alters local redox conditions through water radiolysis [3]. The interaction of α-radiation with water generates several reactive species, including oxidants like H_2O_2 and O_2, as well as reductants such as H_2. These species can significantly influence the redox chemistry at the fuel–water interface.

Over repository timescales, α-decay becomes the dominant source of radiation as the contributions from short-lived β- and γ-emitters decline. The molecular products of α-radiolysis, especially hydrogen and hydrogen peroxide, play opposing roles: while H_2O_2 promotes oxidative dissolution of UO_2, molecular hydrogen can counteract oxidation processes by consuming radiolytic oxidants or through catalytic reactions on metal or oxide surfaces [4–6].Several experimental and modelling studies have shown that hydrogen plays an important role in suppressing the oxidative dissolution of spent nuclear fuel [7–10].

The leaching of spent fuel in presence of corroding iron shows that the interaction between these species (Fe corrosion products, dissolved Fe(II) and molecular hydrogen) has a major impact on the long-term redox stability of spent fuel. In the engineered barrier systems proposed for the Swedish KBS-3 repository concepts, the fuel is encapsulated within copper canisters containing a cast-iron insert. Any localized breach of the canister would result in anoxic corrosion of iron, producing both Fe(II) ions and molecular hydrogen. These corrosion

* Corresponding author.
E-mail address: gidam@chalmers.se (M. Saleh).

https://doi.org/10.1016/j.nme.2026.102148
Received 18 April 2026; Received in revised form 21 May 2026; Accepted 25 May 2026
Available online 26 May 2026

products can alter redox conditions by reacting with oxidizing radiolysis products, thereby influencing the oxidative dissolution of the fuel matrix [11–13].

In a previous study, we investigated the behavior of an unirradiated MOX fuel pellet with 10 wt% Pu under anoxic conditions in simulated Forsmark groundwater in the presence of metallic iron. The results demonstrated that corrosion of iron generated a hydrogen pressure of approximately 2 bars at the end of the more than one year long and Fe (II) concentrations in the 10^{-4}–10^{-3} M range [14]. Under these conditions, uranium release from the MOX pellet was minimal and consistent with the solubility limit of UO_2 (am), indicating that the redox environment produced by anoxic iron corrosion was sufficient to suppress oxidative fuel dissolution, even in the presence of a high α-radiation field. While these findings confirm the strong mitigating role of the corroding iron, the individual contributions of dissolved Fe(II) and molecular hydrogen remain to be clearly defined. From a repository perspective, the period with actively corroding iron stretches to a few ten thousand years (depending on the canister wall thickness and the corrosion rate), while the following period with only corrosion products and a much less active fuel stretches during the whole safety analysis period, usually 10^6 years. For this reason, we tested the leaching of the unirradiated MOX pellet in the presence of two typical anoxic corrosion products of iron, magnetite (Fe_3O_4) and chukanovite ($Fe_2(OH)_2CO_3$), for the reasons described below.

Magnetite is a very stable and ubiquitous anoxic corrosion product of iron. Magnetite has been shown to be the major anoxic iron corrosion product formed in granitic groundwaters over the long term [13,15–18]. In several recent spent fuel leaching studies in the presence of metallic iron [11,12,14] in which relatively high Fe(II) concentrations (10^{-4}-10^{-3}M) were observed, a solid hydroxycarbonate of Fe(II) named chukanovite ($Fe_2(OH)_2CO_3$) has been reported to form.

We synthesized this phase according to the two main synthesis routes reported in the literature and equilibrated it with synthetic Forsmark groundwater and measured relatively high Fe(II) concentrations in equilibrium. Recently, chukanovite $Fe_2(OH)_2CO_3$ has been reported in various studies as a corrosion product of carbon steel [19–21] and was also detected in archaeological objects extracted from anoxic waterlogged soils [22–24] and in zerovalent iron RPB (Reactive Permeable Barriers), used for treatment of contaminated water [25,26]. Initially, this iron corrosion product was named “basic ferrous carbonate” [27] when identified in the corrosion layer of the steel valve of a hot water exchanger. Its crystal structure was similar to that of malachite $Cu_2(OH)_2CO_3$. Later, it was reported to form as a biogenic reduction product of Fe(III) oxyhydroxides instead of cation excess fine-grained magnetite and was named ferrous hydroxycarbonate (FHC) [28]. In 2005 the International Mineralogy Association approved the mineral name “chukanovite” for an iron hydroxide carbonate $Fe_2(OH)_2CO_3$ occurring in a corroding iron meteorite found near Dronino (Russia) [29]. A structural study of this natural chukanovite mineral confirmed that it belongs to the rosasite-malachite group [30], which gathers hydroxy-carbonates with the general formula $A_2(OH)_2(CO_3)$ or AB $(OH)_2(CO_3)$ where A and B are Co, Cu, Fe, Mg, Ni and Zn.

The present study aims to address this knowledge gap by synthesizing Fe(II)-bearing compounds capable of producing aqueous Fe(II) concentrations comparable to those measured in our previous autoclave experiments, and by examining the dissolution behavior of MOX fuel in their presence.

Magnetite was also investigated, as it is one of the major corrosion products formed during iron corrosion under anoxic conditions. This work aims to better understand the respective roles of iron corrosion products, such as magnetite and chukanovite, in maintaining reducing conditions in the near-field of spent nuclear fuel, as well as any role H_2 may play, thereby contributing to a deeper understanding of fuel stability under repository-relevant conditions.

2. Materials and methods

2.1. Materials

2.1.1. Unirradiated MIMAS-MOX fuel

An unirradiated mixed oxide (MOX) fuel pellet containing 10 wt% plutonium was utilized in this study. The pellet was fabricated at the MELOX facility in Marcoule, France, using the MIMAS (MIcronized MASterblend) process. It exhibited approximately 95 % of its theoretical density and possessed a specific alpha activity of 1.79 GBq/g as of August 2023.

For the present experiments, a section of the original MIMAS-MOX pellet was prepared by cutting it into two slices. The portions used in the magnetite and chukanovite experiments weighed 1.6657 g and 1.6565 g, respectively, both maintaining cylindrical geometry. The detailed composition of the fuel is reported in our previous publication [14].

The MIMAS-MOX fuel exhibits a heterogeneous microstructure consisting of three distinct zones that differ in plutonium concentration due to the manufacturing process: (i) a UO_2 matrix-dominated zone, (ii) plutonium-rich agglomerates, and (iii) a coating zone. Additional characterization and compositional information for a comparable MIMAS-MOX fuel containing 7.48 wt% Pu is available in references [12,31,32]. Before leaching experiments, the MOX fuel pellets were annealed for 5 h in a high-temperature graphite furnace (Thermal Technology 1000–2560-FP20) housed within an inert-atmosphere glove box. The annealing treatment was conducted under Ar + 5 % H_2 at 1200 °C, with a heating and cooling rate of 20 °C min^{-1}.

2.1.2. Magnetite and chukanovite

Commercial magnetite was used in this study (Sigma Aldrich, < 5 μm mesh). The chukanovite was synthesized and characterized before its use in the leaching experiments. Chukanovite was synthesized by using the two main methods reported in literature: Mixing of three components $FeCl_2$ (98 % purity, Sigma-Aldrich), Na_2CO_3 powder (99.999 % trace metal basis, Sigma-Aldrich) and carbonate free Titrisol NaOH ampoule (Sigma Aldrich) solutions, or two components (Na_2CO_3 and $FeCl_2$).Both magnetite and chukanovite were selected to represent iron corrosion products expected to form under repository-relevant conditions. For each experiment, 10 g of the respective solid was used. The synthesis of the chukanovite according to the two main methods reported in the literature [33–35] and its characterization are described in some detail in the Supplementary Material, with XRD (with other analytical techniques) analysis confirming the formation of chukanovite with limited crystallinity, as indicated by the presence of characteristic diffraction peaks together with significant background broadening/noise.

2.1.3. Autoclave

Leaching experiments under an argon atmosphere were performed using a modified Parr 4760 Stainless steel autoclave (Parr Instrument Co.) as shown in Fig. 1. The autoclave has a total internal volume of 1 L, capable of withstanding pressures up to 131 bar and temperatures up to 350 °C. Separate experiments were conducted for magnetite and chukanovite leaching tests. The autoclave lid was equipped with two valves to enable liquid sampling and gas purging with Swagelok VCR (Vacuum Coupling Radiation) fittings ensuring a high degree of leak tightness. A digital manometer (WIKA, CPG 1500) protected by a rubber cap was used to continuously monitor pressure during the experiments. Graphite gaskets (coated with a thin layer of silicon grease) were seated in the lid groove and compressed when the lid screws were tightened, forming a gas-tight seal. These gaskets were not reused for subsequent experiments. To minimize contact between the autoclave steel and the reactive materials, a fitted glass beaker insert was employed, containing the leaching solution, MOX pellet, and magnetite or chukanovite, along with the sampling dip tube.

Fig. 1. Image of the autoclave used for the leaching test.

Prior to the experiment, the synthetic Forsmark groundwater (see Section 2.2) was placed in the glass beaker and purged with argon for several hours. The autoclave, containing the solution and solid materials, was then sealed in a bench vise with a bolt torque of 40 Nm to achieve uniform tightening. Argon gas was bubbled through the dip tube to flush the headspace, remove residual oxygen, and saturate the solution before starting the experiment. Bolts were tightened in a crosswise pattern to ensure no leakage and complete deformation of the graphite gasket. Custom-made PEEK dip tubes were used to facilitate liquid sampling throughout the leaching tests.

2.2. Synthetic groundwater compositions

The synthetic Forsmark groundwater used in both experiments was prepared using ≥ 99.0 % ACS reagent grade chemicals (Sigma-Aldrich, Merck) dissolved in ultrapure water with a resistivity of 18.2 MΩ.cm (MilliQ Advantage, Merck). The composition of the solution was designed to reproduce the groundwater chemistry characteristic of the Forsmark site in Sweden [36,37]. The concentrations used in the preparation are listed in Table 1.

2.3. Experimental leaching procedure

2.3.1. Leaching in Forsmark groundwater in the presence of magnetite

The leaching experiment conducted in the presence of magnetite was performed at room temperature (21.0 ± 2.0 °C) under an Ar atmosphere using a sealed autoclave (see Fig. 1). The autoclave reactor was designed to be airtight to ensure anoxic conditions throughout the experiment. Before the leaching test, the autoclave was purged to remove residual air and subsequently pressurized to ~ 10 bars using a gas mixture composed of 99.96 % Ar + 0.04 % CO_2. A 670 mL initial solution containing synthetic Forsmark groundwater prepared as described in Section 2.2 was used in this experiment.

The magnetite solid sample was placed in a small beaker with a glass frit bottom, and the MOX pellet was suspended in the autoclave filled with 670 mL of synthetic Forsmark groundwater. The corrosion of the unirradiated MOX pellet in the presence of magnetite in synthetic Forsmark groundwater was carried out for a total duration of 245 days. The evolution of the dissolved Fe(II), Pu, and U concentrations was measured during the entire leaching test by taking samples at different time intervals during the experiment. Samples were collected without opening the autoclave through a liquid sampling valve, due to the overpressure inside the autoclave. About ~ 10 ml of the liquid was withdrawn from the sampling line at each chosen time interval. The first aliquot (~ 5 mL) taken at each sampling occasion was discarded before sampling to rinse the dip tube and the connection to the autoclave lid. Sample solutions were then taken for analysis. All sample solutions analysed throughout the experiment were filtered using a 0.45 μm polypropylene membrane syringe filter.

2.3.2. Leaching in Forsmark groundwater in the presence of chukanovite

The leaching experiment in the presence of chukanovite was conducted at ambient temperature (21.0 ± 2.0 °C) under an argon atmosphere using a sealed autoclave system to maintain strictly anoxic conditions. The synthesized and characterized chukanovite solid sample was placed in a beaker with a glass frit bottom, then inserted in a bottle with synthetic Forsmark groundwater inside the glove box in order to equilibrate the solid. Afterwards, the chukanovite container was transferred inside the autoclave, and the MOX pellet was introduced. Before the start of the experiment, the autoclave was purged to remove residual air and subsequently pressurized to approximately 10 bars with a gas mixture of 99.96 % Ar and 0.04 % CO_2. The autoclave was loaded with 650 mL of synthetic Forsmark groundwater and subjected to a leaching test period of 70 days (with pure chukanovite) and 130 days (for the leaching test with U-contaminated chukanovite). During the leaching experiment, the evolution of dissolved Fe(II), Pu, and U concentrations was monitored through periodic liquid sampling. Solution samples were collected via a dedicated sampling valve without opening the autoclave, utilizing the internal overpressure to extract the aliquots.

At each sampling interval, approximately 10 mL of solution was withdrawn from the sampling line. The initial ~ 5 mL of each draw was discarded to rinse the dip tube and valve connections before collecting the analytical sample. All solutions were subsequently filtered through 0.45 μm polypropylene membrane syringe filters prior to chemical analysis to ensure removal of particulate matter.

2.4. Termination of the leaching experiment in the presence of magnetite and chukanovite

At the end of the MOX leaching experiment in both studies, the autoclave was opened under Ar atmosphere in a glove bag. The corroded

Table 1
Chemical compositions of the synthetic Forsmark groundwaters (concentrations in $mmolL^{-1}$).

ID	Na	K	Ca	Mg	HCO_3	Cl	SO_4	Si	Br	Fe(II)	Sr	pH
02A	96.57	0.93	22.21	10.04	2.07	148.9	5.28	0.22	0.3	0.04	0.1	7.20

MOX fuel pellet and the magnetite or chukanovite used in the experiment were retrieved from the solution, dried on Kimtech wipes and stored under argon atmosphere in the glove box until surface characterizations were carried out on the respective corroded MOX pellet surfaces.

The leaching solution was filtered with a glass funnel and filter paper to separate any magnetite or chukanovite solid from the solution, after which the volume of the filtered leaching solution was determined. The empty glass beaker was filled with 800 ml 0.5 M HNO_3 and left for 24 h in order to release the uranium or plutonium sorbed on the walls of the glass beaker. After the acidification, the glass beaker was emptied, then filled with 800 ml of 2 M HNO_3 and left for another 24 h. Finally, the glass breaker was rinsed with ultrapure water. Solution samples were taken and analyzed for each acidification step and rinse to quantify the total U and Pu sorbed or precipitated on the glass beaker.

The magnetite or chukanovite collected on filter paper and those in the glass frit were allowed to dry, weighed and dissolved in 2 M HNO_3. The resulting solution was analyzed for U and Pu quantification or sorbed by ICP-MS.

2.5. Solution analysis

2.5.1. pH and Eh

The pH of the solution samples collected from the autoclave containing Forsmark groundwater was measured at different time intervals using a combined glass pH electrode calibrated against standard pH buffer solutions. The electrode was calibrated using commercial pH 4 (biphtalate), pH 7 (phosphate), and pH 10 (KCl / H_3BO_3 /NaOH) buffer solutions (Sigma Aldrich). All pH measurements were performed at room temperature, and the measured values are associated with an uncertainty of approximately ± 0.03 pH units.

The redox potential (Eh) of the sampled solutions was measured using a Phenomenal ORP 220 redox electrode. The electrode was calibrated using a Mettler Toledo InLab Redox Buffer solution (+220 mV at pH 7). The measured potentials were corrected relative to the standard hydrogen electrode (SHE) by accounting for the reference electrode potential and temperature dependence according to the manufacturer's specifications. All reported Eh values correspond to room temperature conditions, with an estimated uncertainty of approximately ± 2 mV.

2.5.2. Mass spectrometry (ICP-MS)

Solution concentrations were determined using ICP-MS (Inductively Coupled Plasma Mass Spectrometry) instrument (Thermo Scientific, Model iCAP). For the leaching test in both experiments, ICP-MS was used to measure the total concentration of U, Pu, and Fe. Both U and Pu concentrations were measured in the standard modes (STD), and solution samples were diluted with a dilution factor of 2 using 0.5 M HNO_3 (Suprapur, Merck) containing 2 ppb Bi-209 as an internal standard (from a 10-ppm certified standard stock solution (CPAchem). External calibration series were prepared from a 10-ppm certified standard U stock solution (CPAchem) in the range of 0—–50 ppb.

The Fe concentration in the sample solutions was measured using kinetic energy discrimination (KED) mode to be able to discriminate or minimize matrix-derived polyatomic interferences on Fe isotopes such as ArO^+, ArN^+, and CaO^+ species [38]. The matrix effects were further corrected using external calibrations, blank samples, internal standard normalization, and optimizing collision cell conditions. The filtered sample solutions were diluted by a dilution factor of 50 with 0.5 M HNO_3 (Suprapur, Merck) containing 2 ppb Y as an internal standard (from a 10-ppm certified standard stock solution (CPAchem). External calibration series were prepared from a 10-ppm certified Fe standard stock solution (CPAchem) in the range of 0 – 500 ppb.

All solution samples were analyzed in triplicate for total concentration determination with both instruments. The detection limit for U and Pu is 0.01 ppb, and for Fe is 1 ppb for the ICP-MS instrument.

2.6. Surface characterizations

2.6. 1. Scanning electron Microscopy with energy dispersive X-ray spectroscopy (SEM-EDX)

A Hitachi TM3000 tabletop scanning electron microscope (SEM) equipped with an energy-dispersive X-ray spectroscopy (EDX) detector was used to analyze the surface of the MOX fuel pellet. The instrument was installed inside an argon-filled glovebox and operated in high-vacuum mode at an accelerating voltage of 30 kV. Due to the radiological activity of the MOX pellet, all SEM-EDX analyses were conducted within the glovebox. Before analysis, the pellet was dried under an inert atmosphere and mounted on carbon tape. SEM-EDX measurements were performed to characterize the surface microstructure and elemental composition of the pellet.

The synthesized chukanovite precipitates were analyzed using a Quanta 200 Environmental SEM (ESEM) equipped with a Schottky field emission gun (FEG) and an Oxford INCA EDX system. The microscope was operated in high-vacuum mode at an accelerating voltage of 20 kV. Dried precipitates were mounted on carbon tape and examined to determine their microstructure and elemental composition. EDX spectra and elemental maps were acquired at multiple locations to assess the compositional homogeneity of the samples.

2.6.2. Powder X-ray diffraction (P-XRD)

X-ray diffraction (XRD) was used to characterize the crystalline structure of magnetite and the synthesized chukanovite. Measurements were carried out using a BRUKER D2 PHASER diffractometer equipped with a monochromatic detector.

Monochromatic Cu Kα radiation (λ = 1.54184 Å) was used for the magnetite, while Mo Kα radiation (λ = 0.7107 Å) was employed for chukanovite measurements. The instrument is equipped with a LYNXEYE detector. Data were collected over a 2θ range of 20°–90°, with the instrument operated at 30 kV and 10 mA. Phase identification and structural refinement were carried out using Diffrac.TOPAS software (version 6.0, Bruker).

3. Results

3.1. Results for the MOX leaching experiment in the presence of magnetite

3.1.1. Measured pH and Eh

The pH of the solution, measured in the presence of magnetite, ranged from 7.2 (± 0.1) to 7.1 (± 0.1), with only a slight decrease in pH observed throughout the duration of the leaching experiment. The redox potential (Eh) measurements were conducted on the sampled solutions at the start and towards the end of the MOX leaching experiment. At the start, corresponding to the first and second data points, Eh ranged from approximately −178 mV to −162 mV/SHE. For the subsequent measurements (last five data points), Eh increased to a range of – 30 mV to –22 mV/SHE. While these measurements showed some instability, they all correspond to reducing conditions, even though the U concentration in solution increased from ~ 10^{-8} M at the start of the experiments to ~ 10^{-6} M at the end of the leaching experiment. The Pt redox electrode is sensitive both to the Fe(II)/Fe(III) couple and to U(VI)/U(IV) couple, hence the observed redox potential and the drift towards more positive potentials show conditions where U(VI) carbonate complexes become significant in solution. With the near neutral pH measured throughout the experiment and bicarbonate (~2 mM) present in the synthetic groundwater composition, U(VI)-carbonate complexes such as $UO_2(CO_3)^{2-}$ and $UO_2(CO_3)_3^{4-}$ are increasingly stable and mobile under mildly reducing to near neutral redox conditions. We have shown previously [14] that Ca-uranyl carbonate complexes dominate for the calcium concentrations typical for Forsmark groundwater.

3.1.2. Evolution of the concentrations of U, Pu, and Fe during the leaching with magnetite

The evolution of uranium, plutonium, and iron concentrations was monitored during the leaching of a MOX pellet in Forsmark-synthesized groundwater in the presence of magnetite (Fe_3O_4). The leaching experiment was conducted under an argon atmosphere to ensure anoxic conditions. The concentrations of U and Pu in solution were determined by inductively coupled plasma mass spectrometry (ICP-MS). Both elements were monitored throughout the experiment as indicators of the oxidative dissolution behavior of the MOX pellet. As shown in Fig. 2, the uranium concentration in solution initially increased from 2.10^{-8} M to 4.10^{-6} M within 50 days of leaching. Thereafter, the U concentration increased much more slowly until the end of the experiment (250 days), indicating that a steady state concentration had been reached. The dissolved plutonium concentration exhibited a similar trend to that of uranium, with an initial increase followed by a much slower increase at later stages of the experiment. The iron concentration decreases with time from 4.10^{-5} M at start to 4.10^{-6} M after 40 days, and drops even lower after 159 days.

These data show that the concentrations of Fe(II) produced by magnetite equilibrated with Forsmark groundwater were not sufficient to counteract the strong alpha field of the unirradiated MOX pellet. Radiolytic dissolution caused the increase of the concentrations of U due to the production of U(VI) and its subsequent release in solution as U(VI) carbonate complexes. The Fe(II) concentrations were relatively low, and the Fe(II) front did not reach the surface of the pellet. Pellet characterization after leaching showed no signs of Fe(III) precipitates on its surface, only NaCl crystals were observed, formed through solution evaporation. In any case, the concentrations of U increased less in our case than in a similar experiment with spent nuclear fuel [13], probably due to the absence of gamma radiation in our case, which caused a slower decrease of Fe(II) concentrations in bulk solution as compared to the spent fuel case. The continuous production of radiolytic oxidants consumes Fe(II) from solution at a higher rate than is partly substituted by magnetite equilibration during the whole test. Towards the end of the test, this higher consumption causes a decrease in Fe(II) concentration. The same radiolytic oxidants oxidize Pu to higher oxidation states (Fe(II) reduces Pu(IV) to Pu(III)), thus when Fe(II) concentrations decrease, the concentration of Pu increases. The final [Pu] ~ 10^{-7} M indicates, very probably, the presence of Pu(V) in solution.

3.1.3. Analysis of the distribution of U and Pu in aqueous solution and sorbed/precipitated on solid surfaces

To quantify the total uranium released in the system containing magnetite and the MIMAS-MOX pellet, the uranium distribution across various system components was assessed at the conclusion of the leaching experiment. Fig. 3 illustrates the partitioning of uranium into soluble fractions, sorbed or precipitated fractions on the quartz beaker insert within the autoclave reactor, and onto the surfaces of the magnetite. The soluble uranium fraction accounted for the majority (86.2 %) of the total uranium released, corresponding to 698.9 μg. The fraction sorbed or precipitated on the quartz beaker insert represents 1.7 % (13.8 μg). The uranium found on magnetite represented 12.3 % of the total uranium released, corresponding to 99.7 μg of uranium. This is in line with the much lower sorption of oxidized U species such as U(VI) carbonate complexes.

In the case of plutonium, 47.5 %, of the total Pu released was sorbed onto the walls of the quartz beaker vessel insert, corresponding to 19.9 μg, while 48.7 % remained in solution (20.4 μg). Only 3.7 % of the total Pu released was sorbed on magnetite, corresponding to 1.6 μg of Pu.

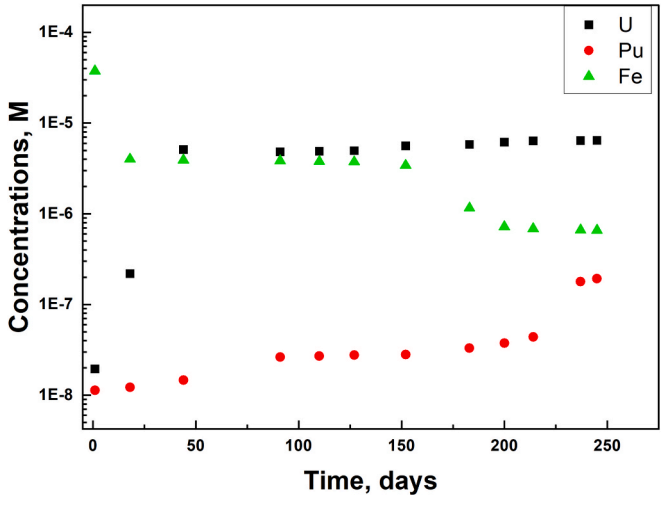

Fig. 2. Evolution of U, Pu and Fe concentrations in solution during leaching of the 10 % Pu MOX pellet under Ar in Forsmark groundwater in the presence of magnetite.

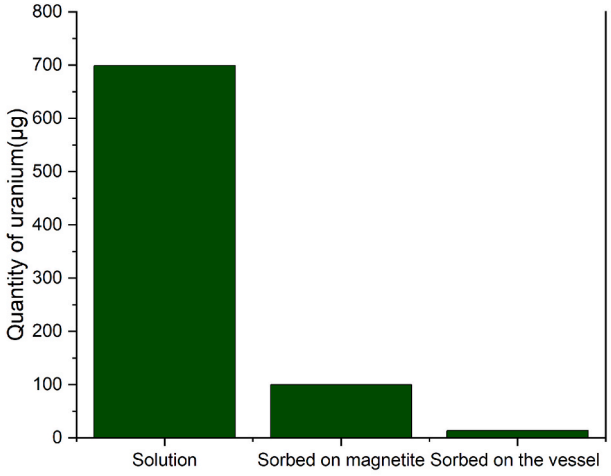

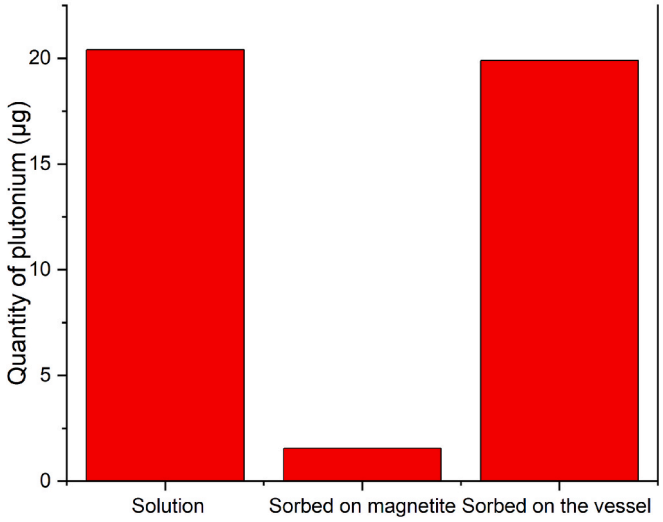

Fig. 3. Uranium and plutonium distribution among the solution, sorbed on the quartz glass beaker insert, and sorbed on the magnetite.

3.2.1. SEM-EDX analysis of the corroded MOX pellet in the presence of magnetite

Fig. 4 shows the surface of the MOX pellet at the end of the leaching test of 245 days in the presence of magnetite. The visual inspection shows the presence of minute whitish precipitates formed on the surface of the leached MOX fuel pellet. The surface of the MOX pellet was investigated by SEM. The SEM micrographs of the surface of the corroded MOX pellet leached in synthetic Forsmark groundwater were acquired using a Hitachi TM 3000 tabletop SEM located in the glove box. Fig. 5 shows the EDX analysis performed on the surface of the corroded MOX fuel pellet, indicating that the precipitates contain Na and Cl originating from evaporation of the synthetic groundwater.

3.2.2. Results of powder X-ray diffraction for magnetite (P-XRD)

The X-ray diffraction analysis performed on the solid magnetite used in the leaching experiment is shown in Fig. 6. The resulting diffractogram reveals distinct peaks, indicating the presence of crystalline phases. The XRD pattern shows narrow and well-defined peaks. The diffractogram was compared against the ICDD database for indexing, yielding matches with expected peaks of magnetite.

3.3. Results of the MOX leaching experiment in the presence of chukanovite

3.3.1. pH and Eh measurements

The pH of the solution, measured in the presence of chukanovite, ranged from 7.2 (± 0.1) to 7.6 (± 0.1), with a gradual increase over the course of the leaching experiment. This increase in pH is attributed to the release of carbonate species from chukanovite, which likely contributed to a higher pH compared to that observed in analogous leaching experiments conducted in the presence of magnetite.

The redox potential (Eh) measurements were carried out on the sampled solutions at the start and towards the end of the MOX leaching experiment. At the start, corresponding to the first three data points, the Eh values ranged from approximately − 102 mV to − 106 mV/SHE. For the subsequent measurement (last two data points), Eh decreased further to approximately − 116 mV, indicating increasingly reducing conditions.

3.3.2. Evolution of the concentrations of U, Pu, and Fe in the leaching with chukanovite

The evolution of the total concentrations of U, Pu, and Fe during the leaching of the MOX pellet under Ar in the presence of 10 g synthetized chukanovite is shown in Fig. 7 as a function of leaching time. The uranium concentrations are quite low (2–4 $x10^{-9}$ M), and only a slight decrease is noted during the whole duration of the experiment.

No increase in U concentrations due to its oxidation caused by the strong alpha radiation field of the MOX pellet is observed, and the results are quite similar to those observed during the leaching of the same MOX pellet under Ar in the presence of metallic iron [14]. The relatively high Fe(II) concentrations resulting from the equilibration of the Forsmark groundwater with chukanovite completely cancel the oxidative dissolution caused by the high alpha field of the MOX pellet. The concentrations of Pu are slightly higher than the solubility of PuO_2(am, hyd) reported as $10^{-10.4}$ M in [39]. In any case, in the presence of such high Fe (II), the concentrations of Pu are quite similar to those reported in [40] Rai et al. (2002) for the reductive dissolution of PuO_2(am, hyd) in the presence of 1 mM Fe(II) in solution. The concentrations of Fe(II) remain constant because the amounts of Fe(II) consumed by the alpha radiolysis oxidants (mainly H_2O_2) are substituted by release of new amounts from the chukanovite equilibrium. A relatively thick layer of red Fe(III)oxyhydroxides was observed on the surface of the MOX pellet upon autoclave opening.

3.3.3. Analysis of the distribution of U and Pu in aqueous solution and sorbed/precipitated on solid surfaces in the test with pure chukanovite

The analysis of the acidic solutions used to desorb the radionuclides from various surfaces or to dissolve the chukanovite completely showed that during the whole duration of the test, very small amounts of U (9.86 μg) and Pu (2.03 μg) were mobilized as shown in Fig. 8. The majority of U was sorbed/ precipitated on chukanovite (6.9 μg, about 70 % of the total), while 26.7 % (2.63 μg) was found sorbed on the surface of the glass vessel used as autoclave insert. The part found in solution (0.33 μg) represented only 3.3 % of the total. The majority of Pu (~96 %) was sorbed on the glass vessel surfaces, around 3.6 % was sorbed on chukanovite, and less than 0.5 % was found in the aqueous phase.

3.4. SEM-EDX analysis of the corroded MOX pellet in the presence of chukanovite

Fig. 9 shows the surface of the MOX pellet at the end of the leaching test of 70 days in the presence of chukanovite. A relatively thick layer of red precipitates, Fe(III)oxyhydroxides was observed on the surface of the MOX pellet upon autoclave opening.

The surface of the MOX pellet was examined using SEM. Micrographs of the corroded MOX pellet surface were acquired with a tabletop SEM installed in the glove box. The images revealed the pellet surface was entirely covered by red precipitates with a granular morphology, typically on the order of a few micrometers in size, as shown in Fig. 10. Similar features have been reported in our previous leaching experiments carried out in the presence of metallic iron foils, where the formed precipitates were identified as Fe(III) oxyhydroxides [14].

The dose rate from the Kapton tape pressed on the pellet was too high, probably due to detachment of grains from the pellet since the 70

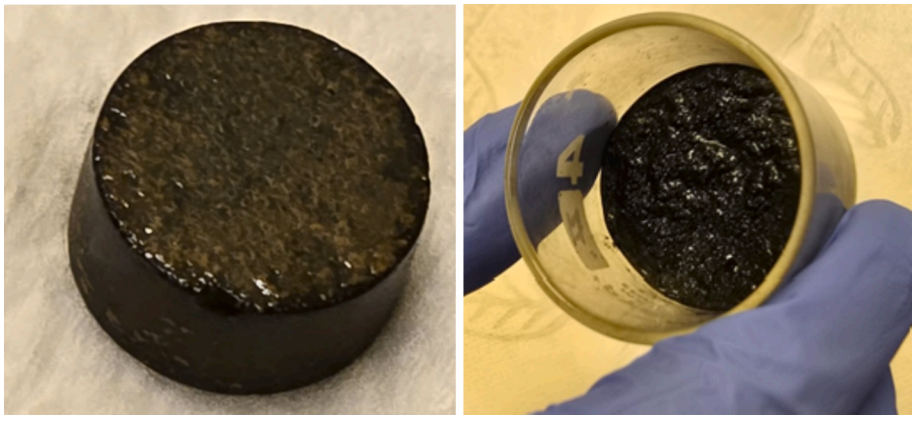

Fig. 4. Visual inspection of the corroded MOX pellet (left) and leached magnetite (right) when extracted from the autoclave. The diameter of the pellet is 8.1 mm, while that of the beaker is 45 mm.

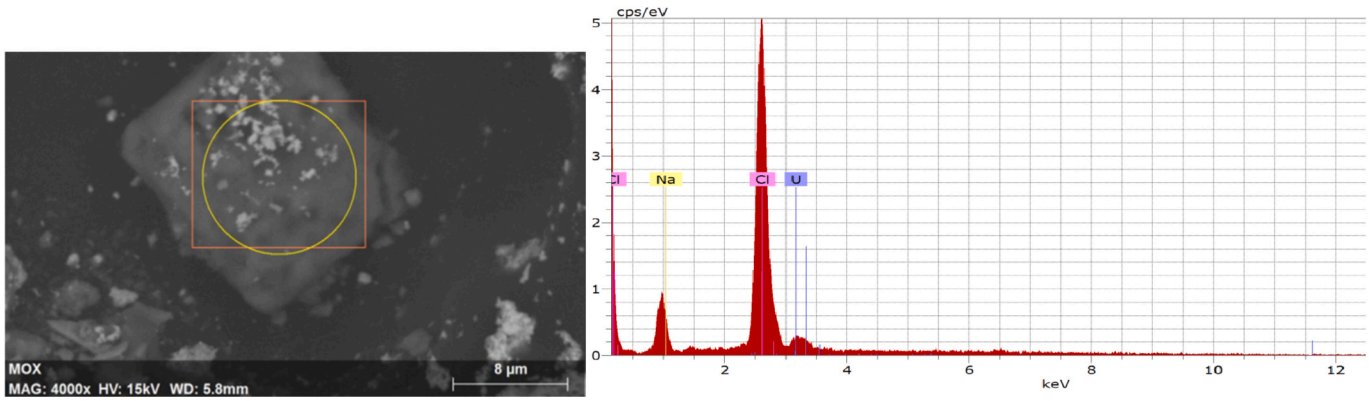

Fig. 5. SEM-EDX analysis of the precipitates formed on the surface of the leached MOX pellet in the presence of magnetite. The yellow circle in the left figure shows the zone investigated by EDX. (For interpretation of the references to colour in this figure legend, the reader is referred to the web version of this article.)

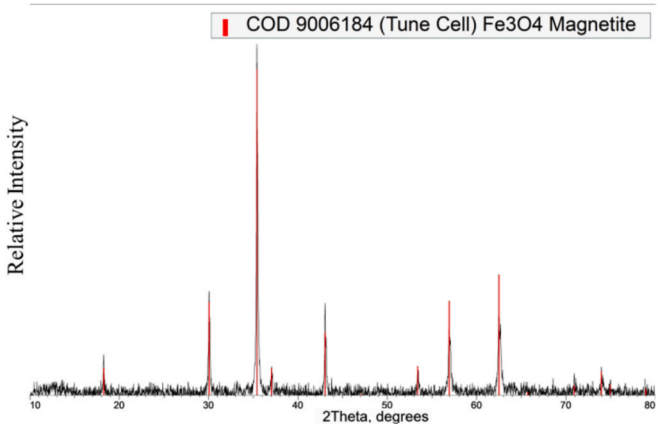

Fig. 6. P- XRD measurement of the magnetite used during the autoclave leaching experiment.

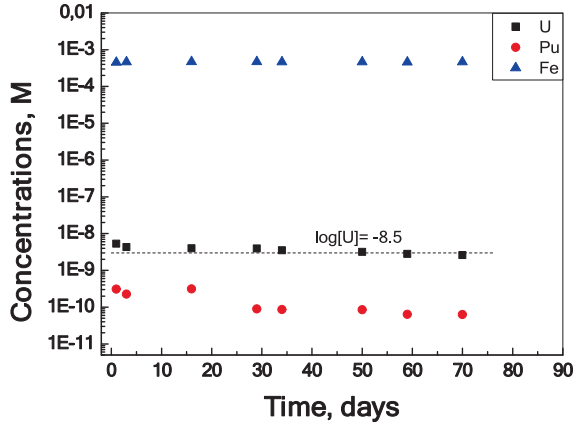

Fig. 7. Evolution of the total concentrations of U, Pu and Fe during the leaching of the 10 wt% Pu MOX pellet under Ar in the presence of chukanovite. The horizontal dotted line indicates the solubility of UO_2(am, hyd) [39].

days layer was not very thick. For this reason, we could not carry out any EDX analysis of the layer deposited on the surface of the pellet.

3.5. *Results of an earlier MOX leaching experiment in the presence of U-contaminated chukanovite*

We carried out an earlier experiment in the presence of chukanovite

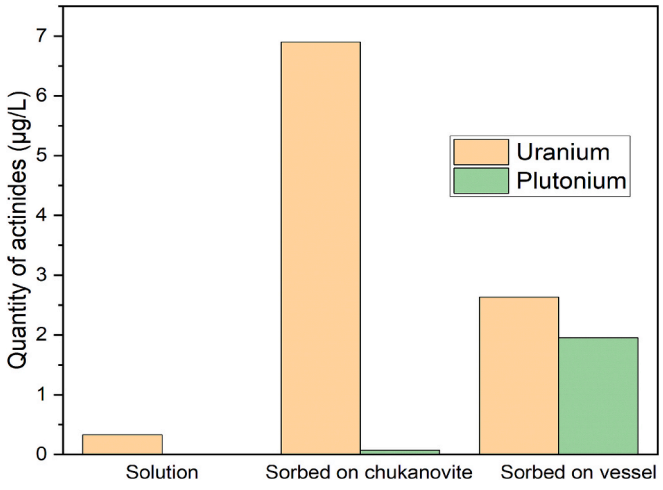

Fig. 8. U and Pu distribution at the end of the leaching test in the presence of chukanovite.

Fig. 9. Visual inspection of the corroded MOX pellet in the presence of chukanovite when extracted from the autoclave. The diameter of the MOX pellet is 8.1 mm.

and discovered only after start that the chukanovite prepared in the

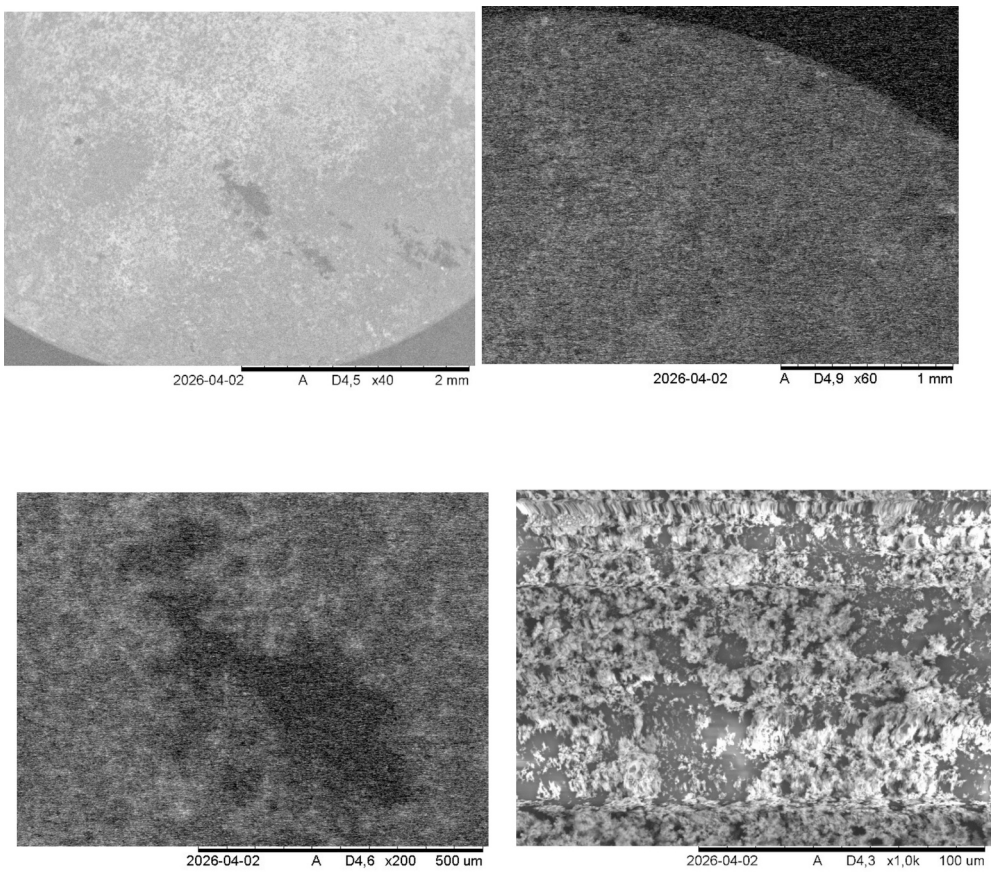

Fig. 10. SEM micrographs of the leached MOX pellet in synthetic Forsmark groundwater in the presence of chukanovite at different magnifications are shown in each figure.

glovebox was contaminated with uranium. We considered interesting to report these results which indicate that chukanovite not only prohibits release of new amounts of oxidized U, but can simultaneously reduce oxidized U resulting e.g. from pre-oxidized fuel layers.

The evolution of the concentrations of U, Pu and Fe in solution during the leaching of the MOX pellet in the presence of 10 g U-contaminated chukanovite is shown in Figs. 11 and 12. As seen from Fig. 11, the concentrations of U are relatively high at start ($3x10^{-6}$ M) and this cannot be due to a pre-oxidized layer on the surface of the MOX pellet, because the pellet was annealed under Ar + 5 % H_2 just before introduction in the autoclave. In any case, the concentration of U does not increase with time as would be expected from the strong alpha radiolysis occurring at the surface of the MOX pellet. It decreases by two orders of magnitude during the first 50 days and continues to decrease with a much slower rate until experiment termination when it reaches $1.2\ 10^{-8}$ M. This decrease is very probably due to the partial reduction of

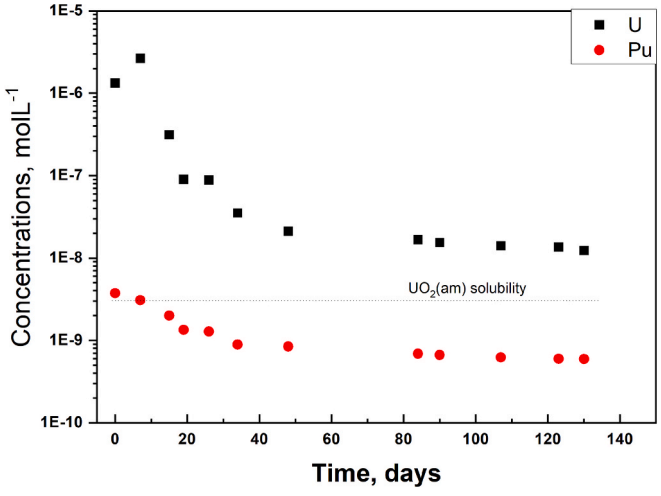

Fig. 11. Evolution of the concentrations of U and Pu during MOX pellet leaching in the presence of U-contaminated chukanovite.

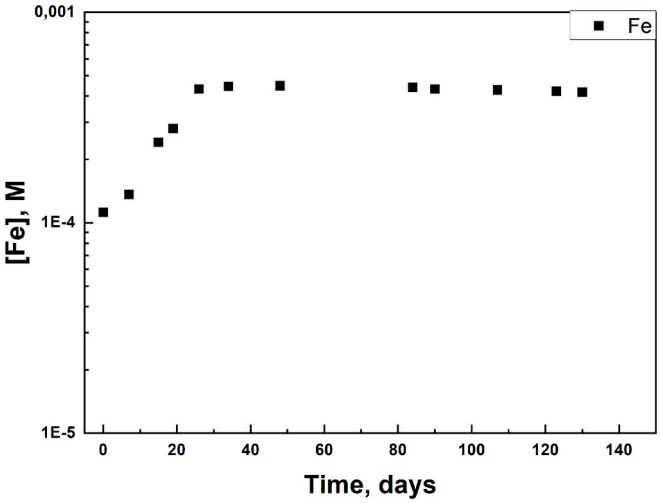

Fig. 12. Evolution of Fe concentrations in solution during leaching of the 10 % Pu MOX pellet under Ar in Forsmark groundwater in the presence of U-contaminated chukanovite.

U(VI) species released from the oxidative dissolution of the pellet or from the chukanovite in the initial stages by Fe(II) ions released by the dissolution of chukanovite. Based on similar arguments as in our previous work [14], we can exclude the precipitation of any U(VI) phase as the cause of the decrease of U concentrations to such low levels. Shoepite (U(VI) hydroxide) has much higher solubilities and Phreeqe C calculations with Thermochimie V.12 SIT database show U concentrations in equilibrium with Forsmark groundwater of 2.8 10^{-4} M for soddyite $(UO_2)_2SiO_4{\cdot}2H_2O$ and 2 x 10^{-4} M for uranophane Ca $(UO_2)_2(SiO_3OH)_2{\cdot}5H_2O$, including the Ca-uranyl-carbonate complexes. Without these ternary complexes, the concentrations of U for soddyite and uranophane in equilibrium with Forsmark groundwater are respectively 9.4x10^{-5} M and 6.3x10^{-6} M, i.e. more than 2 orders of magnitude higher than the final U concentration of 1.2x10^{-8} M. Experimental studies have shown that Fe(II) in solution does not reduce uranyl but does reduce it when sorbed in various surfaces including Fe (III) oxides [41]. The actual experimental data indicates that the reduction by Fe(II) ions of Ca-U-carbonate complexes is relatively fast and continues during the whole duration of the test. The concentrations of Pu decrease slightly in the initial period and then remain constant at similar levels as measured during reductive dissolution of PuO_2(am) in the presence of Fe(II) in solution [40]. The U released from the contaminated chukanovite in the initial period of the test is expected to be reduced by the Fe(II) ion on the surface of chukanovite, as indicated by the strong U accumulation there.

3.5.1. *Analysis of the distribution of U and Pu in aqueous solution and sorbed/precipitated on solid surfaces in the test with uranium-contaminated chukanovite*

To quantify the total uranium released in the system containing chukanovite and the MOX pellet, the U and Pu distribution across various system components was carried out at the end of the leaching experiment of 132 days. Fig. 13 illustrates the distribution of U and Pu into soluble fractions, sorbed or precipitated fractions on the quartz beaker insert within the autoclave reactor, and onto the surfaces of the chukanovite. The soluble uranium fraction accounted for 1.3 % of the total uranium released, corresponding to 2,7 μg. The U fraction sorbed or precipitated on the quartz beaker insert represents 35.7 % (69.2 μg). The majority of the uranium released (63 % corresponding to 122 μg of uranium) was present in the chukanovite. In contrast, Pu exhibited a different distribution. Most of the Pu released 14.4 μg (91.4 %) was sorbed onto the walls of the quartz beaker vessel insert, whereas 1.27 μg was found on the chukanovite. Only 0.3 % of the total Pu released remained in solution, corresponding to 0.1 μg. In total, 193.9 μg of uranium and 15.7 μg of plutonium were released into the system. By comparing these results with the results of the autoclave with non-contaminated chukanovite, it is clear that a large part of the uranium found on chukanovite in this experiment was present there from start. Only 6.9 μg of U was found on the non-contaminated chukanovite test, while in this case most of the 120 μg of U was found on the U contaminated chukanovite have probably been present there from the start.

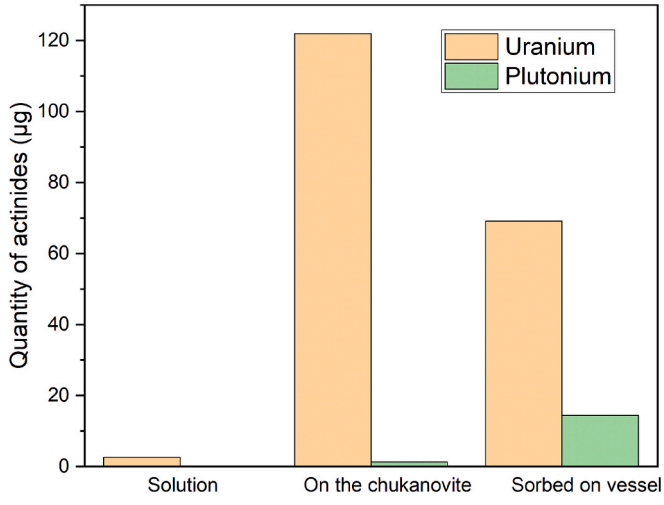

Fig. 13. Uranium and plutonium partitioning among the solution, sorbed on the quartz glass beaker insert, and on the chukanovite at the end of the leaching experiment.

3.5.2. *SEM-EDX analysis of the MOX pellet*

The surface of the MOX pellet was investigated by SEM- EDX at the end of the leaching test of 130 days in the presence of the contaminated chukanovite. The images show that the surface of the pellet is completely covered with red precipitates formed on the surface of the leached MOX fuel pellet, as shown in Fig. 14. The SEM micrographs of the surface of the corroded MOX pellet shows that the surface of the pellet was covered by a μm-sized precipitate with a granular shape (see Fig. 15). The EDX analysis carried out on the surface of the corroded MOX fuel pellet shows that the precipitates contain mainly Fe and O as the major elements in the compounds formed, with no traces of uranium observed in any of the spectra analyzed as shown in Fig. 16. The SEM-EDX analysis suggests that the precipitates primarily consist of Fe-containing compounds, which formed at the fuel/ water interface through the oxidation of Fe(II) to Fe (III). Recent similar studies carried out on MOX fuel in the presence of metallic iron have shown that iron hydroxides such as akageneite (β-FeOOH) tend to precipitate on the surface of the leached MOX pellet [11,12,14].

4. Discussion of results

The relatively low Fe(II) concentrations resulting from equilibration of magnetite with Forsmark groundwater were not sufficient to counteract the extremely high alpha field of the MOX pellet, as shown by the sharp initial increase of the U concentrations in the initial stages of the test. The increase of U concentrations in the later stages of the test is slower, and several factors can contribute to this. Scott et al. [42] have reported that the reduction of U(VI) on the surface of magnetite is accompanied by the oxidation of one Fe(II) on the surface to Fe(III). On the other hand, the relatively low K_d for uranium sorption on magnetite found here and elsewhere indicates that this process is not very important.

The analysis of the distribution of the released U and Pu during the leaching in the presence of magnetite confirms oxidizing conditions during the leaching indicated by the low amount of U sorbed/precipitated on magnetite. The calculated K_d for uranium sorption on magnetite results 6.6 ml/g, which is quite similar to the values reported by Puranen et al. [13] for sorption on magnetite and those reported by Li and Kaplan [43] for the sorption of U(VI) on magnetite. The strong sorption of Pu on the glass vessel walls indicates that it is probably Pu(IV) species that have sorbed, while any oxidized Pu species which can be assumed based on the measured Pu concentrations, have not been reduced on magnetite, given the small amount of Pu sorbed there.

The relatively high Fe(II) concentrations resulting from equilibration of synthetic chukanovite with Forsmark groundwater were sufficient to counteract the extremely high alpha field of the MOX pellet, indicating that the influence of H_2 produced during iron corrosion, if any, is impossible to detect. The total amount of mobilized U in this experiment was very small (9.86 μg) and this indicates that the majority of U found in the U-contaminated chukanovite at test termination was present there from start.

The distribution of the released U and Pu in the presence of chukanovite is in line with reducing conditions. Only a very small part of U and Pu are present in solution, most of U is found sorbed/precipitated on chukanovite while the strong sorption of Pu on the glass vessel is in line with the strong sorption of Pu(III) species.

The relatively high Fe(II) concentrations produced in equilibrium

Fig. 14. Visual inspection of the corroded MOX pellet (left) and leached U-contaminated chukanovite (right) when extracted from the autoclave at the end of the experiment. The diameter of the MOX pellet and the beaker is the same as in Fig. 4.

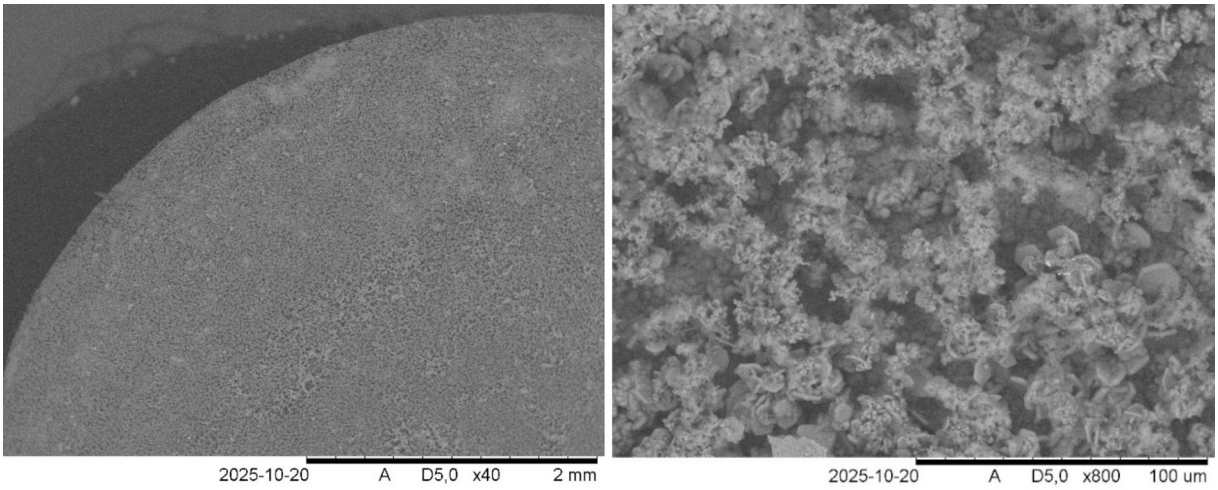

Fig. 15. SEM micrographs of the leached MOX pellet in synthetic Forsmark groundwater in the presence of U-contaminated chukanovite.

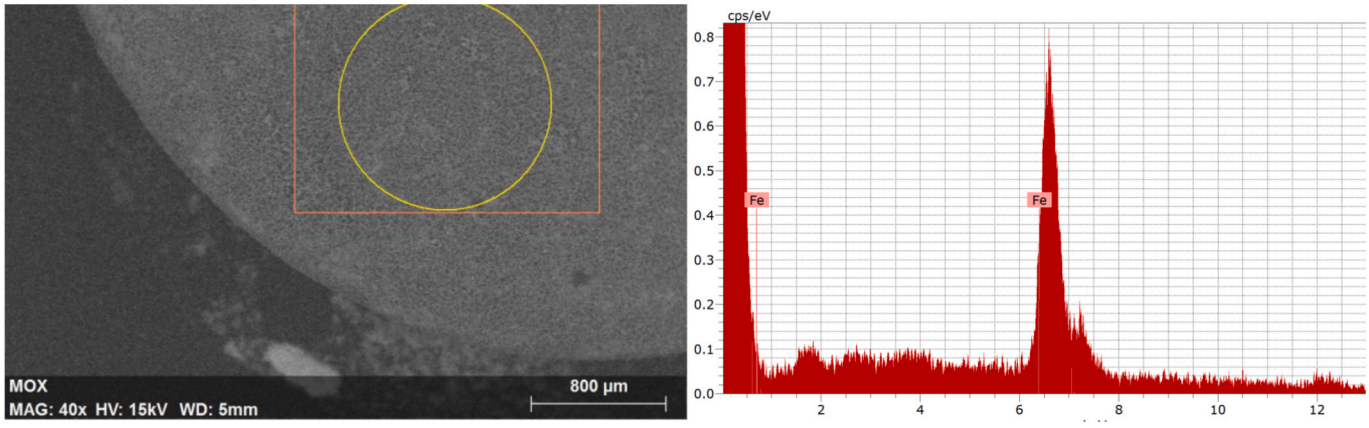

Fig. 16. EDX analyses of the precipitates formed on the leached MOX pellet surface in the presence of U-contaminated chukanovite.

with chukanovite affect not only fuel dissolution, but also radionuclide speciation. For example, any Pu(IV) released in solution will be reduced to Pu(III) in the presence of Fe(II) ions, as shown experimentally by Rai et al. [40].

The spontaneous homogeneous precipitation of Fe(II)-carbonate solids from anoxic solutions is strongly inhibited by kinetic barriers [44,45] and is not expected to affect Fe^{2+}(aq) availability. A recent study shows that at comparable solution saturation at 25 °C, siderite growth rate is nearly 7 orders of magnitude slower than that of calcite [45]. However, recent investigations of Fe(II)-mineral precipitation

mechanisms suggest that heterogeneous nucleation of amorphous Fe-(hydroxy) carbonates, via a multi-step precipitation pathway, may be important in controlling Fe^{2+}(aq) availability [44,46]. This process is initiated by the energetically favorable precipitation of an amorphous Fe-carbonate (AFC), which then provides a reactive surface area on which to promote secondary heterogeneous nucleation of crystalline (hydroxy) carbonate phases in the form of siderite and/or chukanovite. When the ratio of $[CO_3^{2-}]$ to $[Fe^{2+}]$ is high (ratio of activities > 0.725), siderite is the dominant product, while when it is low, chukanovite is favoured [44]. This is because the ratio CO_3^{2-}/Fe^{2+} is much higher for siderite (1.0) than for chukanovite (0.5), and variations of this ratio in solution correspond to variations in saturation state and crystallization rate for both minerals. Chukanovite is considered a metastable phase [45,47] as the thermodynamic equilibrium favors its conversion to siderite by the reaction:

$$Fe_2CO_3(OH)_2 + HCO_3^- + 3H^+ \rightleftarrows 2FeCO_3 + 2H_2O \quad (1).$$

During the corrosion of iron under anoxic conditions, the oxidant is water (H_2O/H^+), and its reduction produces OH^- species. At the corrosion potential, the production of two OH^- ions accompanies the production of a Fe^{2+} cation, and in groundwater containing HCO_3^-/CO_3^{2-} all components necessary for chukanovite formation are present. As long as the metallic iron of the canister insert continues to corrode in the repository, the formation of chukanovite in groundwaters with moderate concentrations of carbonate, as in granitic or clay groundwaters, becomes probable, and the relatively high pH caused by iron corrosion helps in its stabilization. As noted by Lee and Wilkin [26], chukanovite is often encountered as a corrosion product in zerovalent iron PRB, while siderite is never reported. As mentioned in the introduction, chukanovite is reported to form during corrosion of iron under anoxic conditions in repository-related studies or archaeological objects in anoxic environments. Azulay et al. [47] have compared chukanovite stability with that of $Fe(OH)_2$(s) and predict chukanovite precipitation for $[Fe^{2+}] = 10^{-4}$ mol L^{-1}, carbonate activity 0.001 mol L^{-1} for pH > 7.91, and to be stable with respect to $Fe(OH)_2$(s) up to pH = 10.23. The driving force for chukanovite transformation to siderite is important in neutral to acidic conditions and almost null at pH > 11. Only when all the iron is corroded and does not contribute more to the pH increase in the corroding surface, the transformation of chukanovite to siderite or magnetite becomes feasible, especially at lower pH.

Further work should address the long-term aging behavior of chukanovite to support its importance for repository performance assessments. This includes investigating its transformation into other phases over time, such as siderite and magnetite, as well as understanding the interactions between these phases and radionuclides under repository-relevant conditions [48].

5. Conclusions

Two methods for the synthesis of chukanovite and its characterization have been tested successfully, and the synthesized chukanovite has been used in the leaching of a MIMAS-MOX pellet containing 10 wt% Pu. In the presence of groundwater equilibrated with chukanovite, very low U and Pu concentrations were measured during the whole leaching test, indicating that the high Fe(II) concentrations successfully counteracted the very high alpha field of the MOX pellet. It is clear that in a deep repository scenario, when spent fuel contacts groundwater only after several thousand years, the alpha field of the fuel will be orders of magnitude lower than that from our MOX pellet, and the effect of chukanovite presence will completely cancel any oxidative fuel dissolution.

Magnetite, on the other hand, produces much lower concentrations of Fe(II) in equilibrium with groundwater, which are not sufficient to counteract the high alpha field of the MOX pellet. In any case, it has been shown experimentally that magnetite can reduce U(VI) from solution [48], and this may be the reason for the slower increase of U concentrations in the later stages of the leaching.

Funding information

This work was supported by the Swedish Nuclear Fuel and Waste management Company (SKB) under Grant number 21235062.

CRediT authorship contribution statement

M. Saleh: Writing – review & editing, Writing – original draft, Visualization, Validation, Methodology, Investigation, Formal analysis, Data curation, Conceptualization. **E. Darwish:** Writing – review & editing, Validation, Investigation, Formal analysis, Data curation. **M. Hedberg:** Writing – review & editing, Visualization, Validation, Supervision, Investigation, Formal analysis, Data curation. **P.L. Tam:** Writing – review & editing, Validation, Investigation, Formal analysis, Data curation. **K. Spahiu:** Writing – review & editing, Visualization, Validation, Supervision, Project administration, Investigation, Data curation, Conceptualization. **C. Ekberg:** Writing – review & editing, Validation, Resources, Project administration, Funding acquisition, Conceptualization.

Declaration of competing interest

The authors declare that they have no known competing financial interests or personal relationships that could have appeared to influence the work reported in this paper.

Acknowledgements

The Swedish Nuclear and Fuel and Waste Management Company (SKB) is greatly acknowledged for funding this research project. The authors wish to thank Katarina Logg from the Chalmers Material Analysis Laboratory (CMAL) for her help during the FT-IR and Raman measurements. The authors also wish to thank Christophe Jegou and Veronique Broudic of CEA, Marcoule, for all their administrative work related to the transport of the MIMAS MOX pellet to Chalmers in 2018, which made this study possible. Finally, the authors would like to thank the reviewers for their valuable comments and suggestions, which helped improve the quality of this work.

Appendix A. Supplementary data

Supplementary data to this article can be found online at https://doi.org/10.1016/j.nme.2026.102148.

Data availability

Data will be made available on request.

References

[1] D.W. Shoesmith, Fuel corrosion processes under waste disposal conditions, J. Nucl. Mater. 282 (2000) 1–30.
[2] Grenthe, I., Gaona, X., Plyasunov, A., L. Rao, L., Runde, W.H.,B. Grambow, Konings, R.J. M. Smith, A.L., Moore, E.E., 2020. Second Update on the Thermodynamics of U, Np, Pu, Am and Tc, OECD Nuclear Energy Agency Data Bank Eds., OECD publications, Paris, France.
[3] J.W.T. Spinks, R.J. Woods, Introduction to Radiation Chemistry, 3rd ed.,, John Wiley & Sons Inc, New York, 1990.An.
[4] L. Liu, I. Neretnieks, The effect of hydrogen on oxidative dissolution of spent fuel, Nucl. Technol. 138 (2002) 69–77.
[5] M. Broczkowski, J. Noël, D. Shoesmith, The inhibiting effects of hydrogen on the corrosion of uranium dioxide under nuclear waste disposal conditions, J. Nucl. Mater. 346 (2005) 16–23.
[6] M. Trummer, M. Jonsson, Resolving the H_2 effect on radiation-induced dissolution of UO_2-based spent nuclear fuel, J. Nucl. Mater. 396 (2010) 163–169.
[7] E. Ekeroth, M. Granfors, D. Schild, K. Spahiu, The effect of temperature and fuel surface area on spent nuclear fuel dissolution kinetics under H_2 atmosphere, J. Nucl. Mater. 531 (2020) 151081.
[8] P. Carbol, P. Fors, S. Van Winckel, K. Spahiu, Corrosion of irradiated MOX fuel in presence of dissolved H_2, J. Nucl. Mater. 392 (2009) 45–54.

[9] M. Jonsson, F. Nielsen, O. Roth, E. Ekeroth, S. Nilsson, M.M. Hossain, Radiation induced spent nuclear fuel dissolution under deep repository conditions, Envir. Sci. Techn. 41 (2007) 7087–7093.
[10] N. Liu, Z. Qin, J.J. Nöel, D.W. Shoesmith, Roles of radiolytic and externally generated H_2 in the corrosion of fractured spent fuel, J. Nucl. Mater. 494 (2017) 87–94.
[11] M. Odorowski, C. Jegou, L. de Windt, V. Broudic, G. Jouan, S. Peuget, C. Martin, Effect of metallic iron on the oxidative dissolution of UO2 doped with a radioactive alpha emitter in synthetic Callovo-Oxfordian water, Geochim. Cosmochim. Acta 219 (2017) 1–21.
[12] C. Jegou, M. Odorowski, V. Kerleguer, V. Broudic, M.L. Schlegel, G. Jouan, C. Marques, L. De Windt, MOX fuel corrosion processes under waste disposal conditions, J. Corr. Sci. 195 (2022) 109964.
[13] A. Puranen, A. Barreiro-Fidalgo, L.Z. Evins, Spahiu, Spent fuel corrosion and the impact of iron corrosion – the effects of hydrogen generation and formation of iron corrosion products, J. Nucl. Mater. 542 (2020) 152423.
[14] M. Saleh, N.L. Hansson, M. Hedberg, K. Spahiu, C. Ekberg, Dissolution of unirradiated MOX fuel in the presence of metallic iron, J. Nucl. Mater. 618 (2025) 156202.
[15] N.R. Smart, D.J. Blackwood, L. Werme, Anaerobic corrosion of carbon steel and cast iron in artificial groundwaters: Part 1-Electrochemical aspects, Corrosion 58 (2002) 547–559.
[16] N.R. Smart, D.J. Blackwood, L. Werme, Anaerobic corrosion of carbon steel and cast iron in artificial groundwaters: Part 2-Gas generation, Corrosion 58 (2002) 627–637.
[17] N.R. Smart, A.P. Rance, L.O. Werme, Anaerobic Corrosion of Steel in Bentonite, Mat. Res. Soc. Symp. Proc. 807 (2004) 441–446.
[18] N.R. Smart, A.P. Rance, L. Carlson, L.O. Werme, Further Studies of the Anaerobic Corrosion of Steel in Bentonite, MRS. Symp. Proc. 932 (2006) 813–820.
[19] T. Nishimura, J. Dong, Corrosion behavior of carbon steel for overpack in groundwater containing bicarbonate ions, J. Power Energy Syst. 3 (2009) 23–30.
[20] J. Dong, T. Nishimura, T. Kodama, Corrosion behavior of carbon steel in bicarbonate (HCO_3^-) solutions, Mat. Res. Soc. Symp. Proc. 713 (2002) 105–112.
[21] M. Schlegel, C. Bataillon, C. Blanc, D. Pret, E. Foy, Anodic activation of iron corrosion in clay media under water saturated conditions at 90 ℃: characterisation of the corrosion interface, Environ. Sci. Technol. 44 (2010) 1503–1508.
[22] M. Saheb, D. Neff, P. Dillmann, H. Matthiesen, E. Foy, Long-term corrosion behavior of low-carbon steel in anoxic environment: characterization of archaeological artefacts, J. Nucl. Mater. 379 (2008) 118–123.
[23] M. Saheb, D. Neff, P. Dillmann, H. Matthiesen, E. Foy, Iron corrosion in an anoxic soil: Comparison between thermodynamic modelling and ferrous archaeological artefacts characterised along with the local in situ geochemical conditions, Appl. Geochem. 25 (2010) 1937–1945.
[24] M. Saheb, D. Neff, L. Bellot-Gurlet, P. Dillmann, Raman study of deuterated iron hydroxycarbonate to assess long term corrosion mechanisms in anoxic soils, J. Raman Spectrosc. 42 (2011) 1100–1108.
[25] T. Kohn, K. Livi, A.I. Roberts, P. Vikesland, Longevity of granular iron in groundwater treatment process: corrosion product development, Environ. Sci. Technol. 39 (2005) 2867–2879.
[26] T.R. Lee, R.T. Wilkin, Iron hydroxide carbonate formation in zerovalent iron permeable reactive barriers: characterization and evaluation of phase stability, J. Contam. Hydrol. 116 (2010) 47–57.
[27] E. Erdös, H. Altorfer, Ein dem Malachit ahnliches basisches Eisenkarbonat als Korrosionsprodukt von Stahl, Werkstofe Und Korrosion 27 (1976) 304–312.
[28] R.K. Kukkadapu, J.M. Zachara, J.K. Fredrickson, D.W. Kennedy, A.C. Dohnalkova, D.E. Maccready, Ferrous hydroxycarbonate is a stable transformation product of biogenic magnetite, Am. Mineral. 90 (2005) 510–515.
[29] E.A.J. Burke, G. Ferraris, New minerals approved in 2005- Nomenclature modifications approved in 2005 by the commission on new minerals and mineral names, International Mineralogical Association, Canadian Mineralogist. 44 (2006) 547–552.
[30] I.V. Pekov, N. Perchiazzi, S. Merlino, V.N. Kalachev, M. Merlini, A.E. Zadov, Chukanovite, $Fe_2(CO_3)(OH)_2$, a new mineral from the weathered iron meteorite Dronino, Eur. J. Mineral. 19 (2007) 891–898.
[31] M. Odorowski, C. Jegou, L. De Windt, V. Broudic, S. Peuget, M. Magnin, M. Tribet, C. Martin, Oxidative dissolution of unirradiated MIMAS MOX fuel (U/Pu oxides) in carbonated water under oxic and anoxic conditions, J. Nucl. Mater. 468 (2016) 17–25.
[32] Z. Talip, S. Peuget, M. Magnin, M. Tribet, C. Valot, R. Vauchy, C. Jegou, Characterization of un-irradiated MIMAS MOX fuel by Raman spectroscopy and EPMA, J. Nucl. Mater. 499 (2018) 88–97.
[33] C. Remazeilles, P. Refait, Fe(II) hydroxycarbonate $Fe_2(OH)_2CO_3$ (chukanovite) as iron corrosion product; Synthesis and study by Fourier Transform Infrared Spectroscopy, Polyhedron 28 (2009) 749–756.
[34] R. Chen, J. Chen, M. Hong, W. Zhang, Formation of chukanovite in simulated groundwater containing CO_3^{2-}, Environ. Techn. 37 (2016) 2786–2792.
[35] R. Kirsch, D. Fellhauer, M. Altmaier, V. Neck, A. Rosberg, T. Fanghänel, L. Charlet, A. Scheinost, Oxidation state and local structure of plutonium reacted with magnetite, mackinawite, and chukanovite, Environ. Sci. and Techn. 45 (2011) 7267–7274.
[36] M. Laaksoharju, J. Smellie, E.L. Tullborg, M. Gimeno, J. Molinero, J. Gurban, L. Hallbeck, 2008.Hydrogeochemical evaluation and modelling performed within the swedish site investigation programme, Appl. Geochem. (1761–1795.).
[37] M. Laaksoharju, J. Smellie, E.L. Tullborg, M. Gimeno, L. Hallbeck, J. Molinero, N. Waber, Bedrock Hydrogeochemistry Forsmark. Site descriptive modelling SDM-Site Forsmark, SKB R-08-47, Svensk Kärnbränslehantering AB (2008).
[38] N. Yamada, Kinetic energy discrimination in collision/reaction cell ICP-MS: Theoretical review of principles and limitations, Spectrochim. Acta B At. Spectrosc. 110 (2015) 31–44.
[39] A.S. Kertes, R. Guillaumont, Solubility of UO_2: a comparative review, Nucl. Chem. Waste Manage. 5 (3) (1985) 215–219.
[40] D. Rai, Y.A. Gorby, J.K. Fredrickson, D.A. Moore, M. Yui, Reductive dissolution of PuO_2(am): the effect of Fe(II) and hydroquinone, J. Soln. Chem. 31 (2002) 433–453.
[41] E. Liger, L. Charlet, P. Van Cappellen, Surface catalysis of uranium (VI) reduction by iron (II), Geochim. Cosmochim. Acta 63 (1999) 2939–2955.
[42] T.B. Scott, G.C. Allen, P.J. Heard, M.G. Randell, Reduction of U(VI) to U(IV) on the surface of magnetite, Geochim. Cosmochim. Acta 69 (2005) 5639–5646.
[43] D. Li, D.I. Kaplan, Sorption coefficients and molecular mechanisms of Pu, U, Np, Am, and Tc to Fe (hydr)oxides: a review, J. Haz. Mater. 243 (2012) 1–18.
[44] C.Z. Jiang, N.J. Tosca, Fe(II) carbonate precipitation and the chemistry of anoxic ferruginous water, Earth Planet, Sci. Lett. 506 (2019) 231–242.
[45] C.Z. Jiang, N.J. Tosca, Growth kinetics of siderite at 298.15 K and 1 bar, Geochim. Cosmochim. Acta 274 (2020) 97–117.
[46] N.J. Tosca, C.Z. Jiang, B. Rasmussen, J. Muhling, Products of the iron cycle on the early Earth, Free Rad, Biol. Med. 140 (2019) 138–153.
[47] I. Azoulay, C. Remazeilles, P. Refait, Determination of standard Gibbs free energy of formation of chukanovite and Pourbaix diagrams of iron in carbonated media, Corr. Sci. 58 (2012) 229–236.
[48] K. Schmeide, A. Rossberg, F. Bok, S.S.A. Azzam, S. Weiss, A.C. Scheinhost, Technetium immobilization by chukanovite and its oxidative transformation products: Neural network analysis of EXAFS spectra, Sci. Tot. Environ. 770 (2021) 145334.